Available online at www.sciencedirect.com

ScienceDirect

Procedia Structural Integrity 23 (2019) 360–365

Structural Integrity Procedia

www.elsevier.com/locate/procedia

9th International Conference on Materials Structure and Micromechanics of Fracture

Failure of Gadolinium Zirconate and Yttria Stabilized Zirconia Thermal Barrier Coatings Subjected to High Temperature Calcia-Magnesia-Alumino-Silicate Attack

Ladislav Čelko[a,*], David Jech[a], Serhii Tkachenko[a], Pavel Komarov[a], Michaela Remešová[a], Karel Slámečka[a], Pavel Ctibor[b]

[a]*CEITEC – Central European Institute of Technology, Brno University of Technology, Purkyňova 123, 612 00 Brno, Czech Republic*
[b]*IPP – Institute of Plasma Physics, Academy of Sciences of the Czech Republic, Za Slovankou 3, 182 00 Prague, Czech Republic*

Abstract

Nowadays, the contribution of rare-earth oxide compounds is extensively investigated with the aim to improve the service life of gas turbine engine components protected by thermal barrier coatings (TBCs) against the environmental Calcia-Magnesia-Alumino-Silicate (CMAS) attack. Therefore, the TBCs consisting of a NiCrAlY bond coat, Yttria Stabilized Zirconia (YSZ) and/or mixture of YSZ and Gadolinium Zirconate (YSZ+GZ) interlayers, and a GZ top coat, which were all deposited by atmospheric plasma spraying onto the nickel-based superalloy substrates, are introduced in this contribution. The CMAS-attack resistance was evaluated using an indirect method. Firstly, the thin layer of CMAS prepared from colloidal solutions was deposited onto the top coat surface and, after drying, the samples were heat treated with the aim to glassified the CMAS. Secondly, the coated samples containing CMAS glass debris were subjected to rapid heating (up to 1200 °C) and enforced cooling cycles at the burner-rig test device and the failure of TBC was investigated. In all cases, the failure mechanism due to the CMAS attack was the top coat spallation. The functional graded TBC was found to be the most resistant system.

* Corresponding author. Tel.: +420-541-14-9701.
E-mail address: ladislav.celko@ceitec.vutbr.cz

2452-3216
10.1016/j.prostr.2020.01.113

Keywords: Atmospheric Plasma Spraying; Thermal Barrier Coatings; Gadolinium Zirconate; Calcia-Magnesia-Alumino-Silicate Glass; High Temperature

1. Introduction

First thermal barrier coatings (TBCs) appeared in the late 70' and TBCs are nowadays widely used in aerospace industry and energetics to protect the critical gas turbine engine components, such as combustion chambers, blades, vanes and liners, against surrounding hot gasses during service. The TBCs usually consist of a Ni or Co-based metallic bond coat, alumina and/or spinel thermally grown oxide, and partially 6-8 wt.% Y_2O_3 stabilized ZrO_2 tetragonal phase as a ceramic top coat. The bond coat and the top coat are predominantly manufactured by means of atmospheric plasma spraying or electron beam physical vapor deposition techniques, as testified by the published works related to the subject: the history, development and manufacturing of TBCs in Bose (2007), and the working principle and structure of TBCs in Padture et al. (2002). In addition to very high temperatures (the hottest section of gas turbine reaches temperatures up to 1200 °C), the TBC materials need to ensure the safety and reliability of coated components also against many other intrinsic and extrinsic factors, as explained in detail in Darolia (2013), such as, for example, (i) undesirable sintering resulting in increase in the top coat thermal conductivity, (ii) undesirable high temperature phase transformations arising from the interaction with vapors from incomplete combustion or air pollution, or (iii) foreign object damage caused by impact of non-melted high-speed solid particles, which may enter through the filtration system. After more than forty years of TBCs in service, the eruption of volcano Eyjafjallajökull in Island on 15th April 2010 enforced the closure of all the airports in Europe due to the ash cloud which damaged most of TBCs, thus significantly influencing the modern aerospace history. The so called Calcia-Magnesia-Alumino-Silicate (CMAS) environmental attack, as described in Steinke et al. (2010), was identified and the related degradation mechanisms were studied for conventional YSZ TBCs in detail at various temperatures in Krause et al. (2016) and in the molten CMAS phase condition in Drexler et al. (2012). As a result of these and other studies, see Čelko et al. (2017), two different failure mechanisms of YSZ TBCs were identified, depending on the temperature. The first, relatively slow mechanism, is observed below the temperature of ~1050 °C and it is related to the depletion of yttria from stabilized tetragonal zirconia phase, forming more stable calcia and silica phases and transforming the yttria depleted zirconia into undesirable monoclinic phase of low thermal cyclic stability. The second mechanism, which is active above the temperature of ~1050 °C, is related to penetration of molten CMAS into the porous top coat structure, its solidification during the cooling period, causing loss of YSZ strain tolerance, and rapid failure of YSZ TBC after the next heating/cooling cycle. Therefore, complex multilayer ceramic systems and/or novel mitigation strategies designed to reduce or block the molten CMAS infiltration, as introduced in Poerschke et al. (2017), aiming to substitute or protect the YSZ ceramic top coat, are extensively investigated.

In the last decade, the multilayer TBCs concept, utilizing rare earth zirconate top coats produced in the form of pyrochlore $X_2Zr_2O_7$ structure, where X means the rare earth element, started to be studied due to the beneficial combination of low thermal conductivity and enhanced CMAS resistance. As published in Schultz and Braue (2013), the $La_2Zr_2O_7$ provides significant but varying potential for mitigation of TBC damage caused by CMAS deposit. The suspension plasma sprayed multilayer TBCs consisting of YSZ – GZ or YSZ – GZ and dense GZ, see Mahade et al. (2017), provided significant improvement of cyclic oxidation life-time in comparison with the single layer YSZ TBC. Moreover, the thin and dense GZ top layer is expected to further improve the multilayer TBC CMAS resistance. The different concept of periodic variation in ceria-yttria stabilized zirconia and GZ thin layers was introduced in Gok and Goller (2017) and such multilayer design was found to prolong the cyclic oxidation life-time in comparison with the single layer GZ TBC.

The objective of this study was to introduce the comparative and new design of multilayer TBCs consisting of (a) thin and dense GZ top coat, and (b) the YSZ+GZ interlayer together with the thin and dense GZ top coat, both deposited on YSZ TBC. Both plasma sprayed multilayer TBCs, were subjected to CMAS environmental attack at the high temperature burner rig cyclic oxidation test. In order to obtain the TBCs response to CMAS attack and to identify the

failure mechanism and undergoing phases transformation, the available techniques for materials science studies were used.

2. Materials and Methods

2.1. Experimental material

Samples of cylindrical shape made from polycrystalline nickel-based superalloy INCONEL® Alloy 718 (Stanford Advanced Materials), were used as a substrate. Surface of each sample was grit-blasted by fused white alumina F280 powder, cleaned by compressed air and washed with acetone in an ultrasonic cleaning bath prior to the deposition of coatings. The NiCrAlY gas atomized powder (80.46.8 – GTV GmbH) with a nominal particle size of 15-38 μm was used for the metallic bond coat. The ZrO_2-$7Y_2O_3$ plasma spherodized HOSP powder (Amperit 831 – H.C. Starck) with a nominal particle size of 45-125 μm and/or a homogeneous powder mixture in 1 : 1 weight-ratio consisting of ZrO_2-$7Y_2O_3$ and $Gd_2Zr_2O_7$ powders were used for ceramic interlayer(s). The $Gd_2Zr_2O_7$ agglomerated and sintered powder (Amperit 835 – H.C. Starck) with a nominal particle size of 45-125 μm was utilized for the top coat.

2.2. Deposition of thermal barrier coatings

All coatings were deposited by means of an atmospheric plasma spray unit MF-P-1000 (GTV GmbH) equipped with a F4MB-XL plasma gun (Oerlicon Metco), utilizing Ar + H_2 plasma gas mixture, and recommended and trend in experimentally developed parameters compare to YSZ that are listed in Table 1.

Two sets of samples were manufactured, i.e. (i) multilayer TBC consisting of ~100 μm thick NiCrAlY metallic bond coat, ~400 μm thick YSZ ceramic interlayer, and ~40 μm thick GZ ceramic top coat, and (ii) functional graded TBC consisting of ~100 μm thick NiCrAlY metallic bond coat, ~200 μm thick YSZ and ~200 μm thick YSZ+GZ ceramic interlayers, and ~40 μm thick GZ ceramic top coat.

Table 1. Deposition parameters of coatings.

Coating material	Ar (slpm)	H_2 (slpm)	Current (A)	Spray distance (mm)
NiCrAlY	65	14	700	140
YSZ	30	3	500	135
YSZ+GZ	↑	↑	↑	↑
GZ	↑	↑	↑	↓

2.3. Deposition of CMAS and testing of CMAS resistance

The top coats of multilayer and functional graded TBCs were brush painted by suspension consisted of deionized water and ultrafine CMAS test dust. According to the aerospace standards, the CMAS layer of a certain thickness was deposited onto the top coat, slowly dried, and subsequently glassified at the temperature above 1250 °C in a laboratory furnace LH 06/13 (LAC).

The burner rig cyclic oxidation test was carried out using a prototype of propane/oxygen flame apparatus (Central European Institute of Technology). The TBCs coated samples after glassification with remaining CMAS debris were subjected to five flame/compressed-air rapid heating/enforced cooling cycles with the maximum temperature of the top coat of 1200 °C. Each cycle consisted of heating in the flame and cooling outside the flame. During the heating part of the cycle, backside cooling was applied to create the constant temperature gradient of the substrate. The burner rig cyclic oxidation test was controlled by means of a single wave pyrometer, utilized to measure the outer surface temperature of coated samples, assuming the constant emissivity of the top coats. The K-type thermocouple welded to the backside of each sample was used to measure the backside temperature of the uncoated superalloy substrate.

2.4. Characterization techniques

The weight of the TBCs coated samples was measured using analytical balances Discovery (Ohaus) (i) in the as-sprayed state, prior to CMAS deposition, (ii) after CMAS deposition, (iii) after CMAS glassification, and (iv) after five burner rig test cycles. Samples for microstructural characterization were cut-out using a deformation free saw Secotom 50 (Struers GmbH). Metallographic samples for observation were prepared by grinding on abrasive papers with intensive water cooling and polishing with diamond pastes. The observation of coating microstructures and acquisition of micrographs were done by using a scanning electron microscope LYRA3 (Tescan) equipped with EDX microanalyser (Bruker). X-ray diffraction was performed using SmartLab 3kW (Rigaku). Diffractometer was set up in Bragg-Bretano geometry using Cu Kα radiation (l = 1.54 Å). The Cu lamp was operated at a current of 40 mA and a voltage of 45 kV. The diffraction was measured in the 2-Theta range from 20° to 90° with step size of 0.01° and speed of 1.5 s/step. Phases were identified from measured diffraction patterns utilizing PDF2 and ICSD databases.

3. Results and Discussion

3.1. As-sprayed thermal barrier coating systems

The cross-section images of the as-sprayed thermal barrier coating systems are shown in Fig. 1. The micrographs reveal a splat-like microstructure typical for atmospheric plasma sprayed coatings. A certain amount of porosity can be observed within the YSZ and YSZ+GZ interlayers, but note that the small pores are unimportant due to fast rate sintering resulting in accelerated deterioration of TBCs properties, as discussed in Lavasani et al. (2019). To follow the CMAS mitigation strategy, the continuous and thin GZ top coats in both TBCs were manufactured to be as dense as possible, with minimum amount of open porosity.

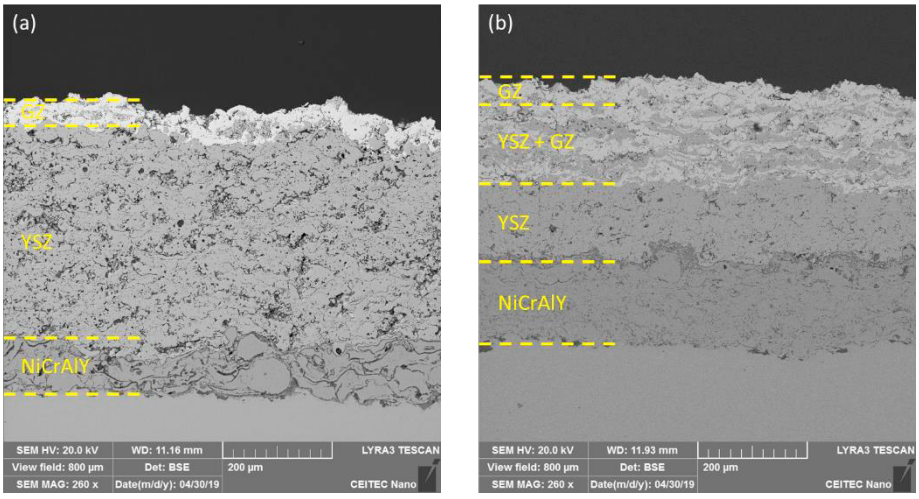

Fig. 1. SEM micrographs of initial-state of (a) multilayer NiCrAlY – YSZ – GZ thermal barrier coating, and (b) functional graded NiCrAlY – YSZ – YSZ+GZ – GZ thermal barrier coating.

3.2. Thermal barrier coating systems after CMAS attack

During cooling from the CMAS glassification temperature down to the room temperature, intensive spallation of CMAS glass from the top coat surface occurred. The thicker CMAS layer found mostly at the sample edges spall out first at moderate temperature in a form of larger plates, followed by a local flake-like spallation from the sample central part during cooling to the room temperature. The weight of both multilayer and functional graded TBCs

decreased after glassification (in comparison to the initial as-sprayed state), the weight loses being 0.38 g and 0.12 g, respectively. Second significant drop in weight occurred continuously via spallation during five cycles at the burner rig test, the weight loses being 0.27 g for the multilayer TBC and 0.14 g for the functional graded TBC. Nevertheless, considering the appearance of the top coat surface, as shown in Fig. 2, and the total weight loss (0.65 g and 0.26 g for multilayer and functional graded systems, respectively) of samples after the CMAS attack, both systems are better than the conventional YSZ TBC tested at the same conditions, which was significantly damaged down to the bond coat.

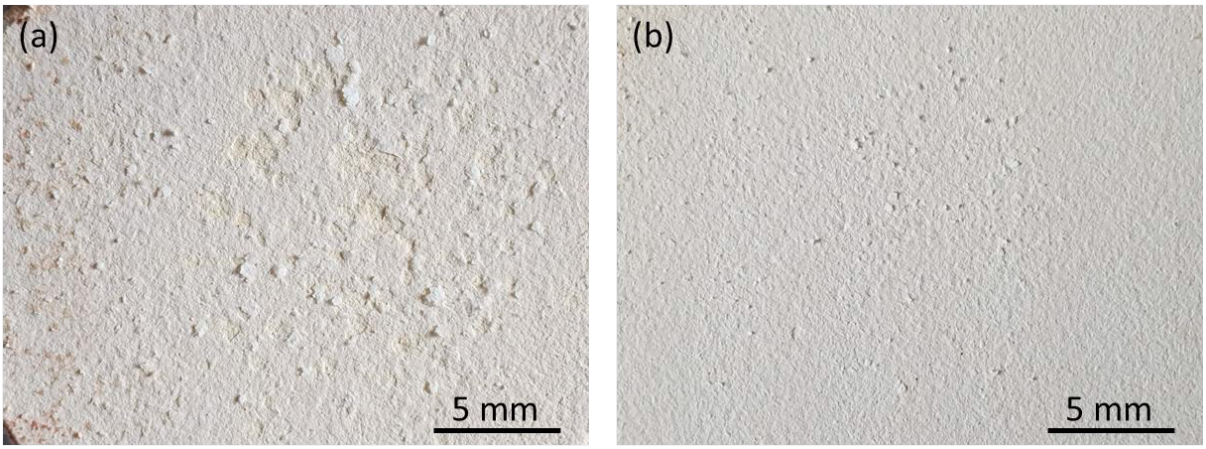

Fig. 2. Macrographs of CMAS environmental attack interaction with (a) multilayer NiCrAlY – YSZ – GZ; and (b) functional graded NiCrAlY – YSZ – YSZ+GZ – GZ thermal barrier coating systems after burner-rig test.

Both as-sprayed TBCs top coats consisted of a single $Gd_2Zr_2O_7$ pyrochlore phase, as shown in Fig. 3, without any other secondary phases that are often formed during plasma spraying due to interactions with surrounding atmosphere.

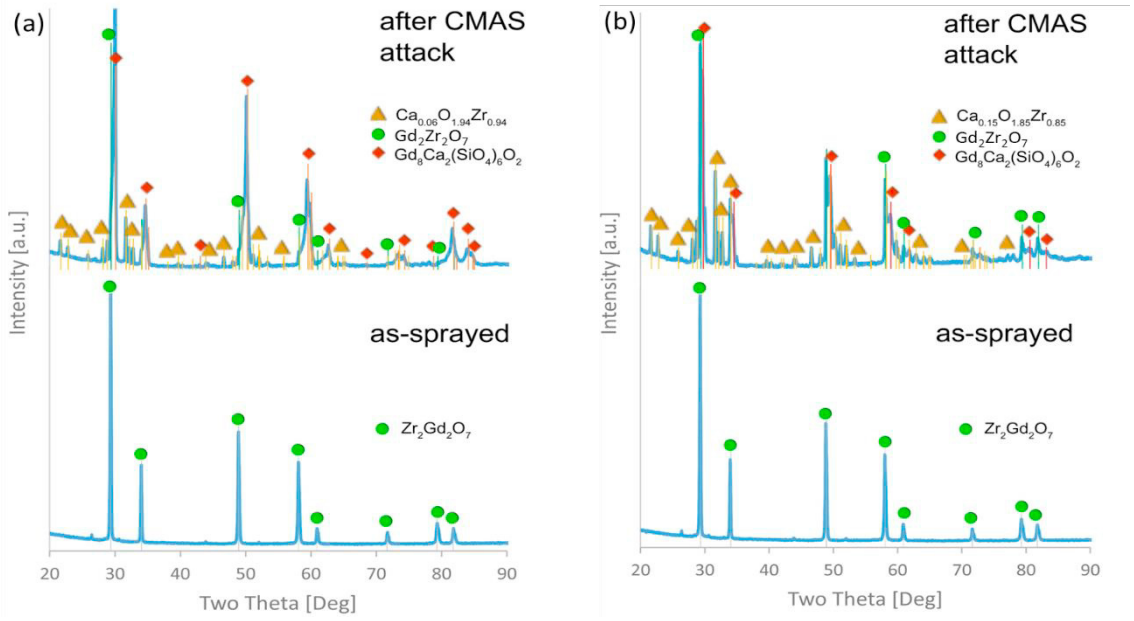

Fig. 3. XRD patterns of as-sprayed and CMAS attacked (a) multilayer NiCrAlY – YSZ – GZ; and (b) functional graded NiCrAlY – YSZ – YSZ+GZ – GZ thermal barrier coating systems.

After CMAS attack, the majority of non-spall out GZ pyrochlore phase was transformed to zirconium calcium oxide and defect fluorite $Gd_8Ca_2(SiO_4)_6O_2$ phases. The difference in stoichiometry of zirconium calcium oxide phases formed ($Zr_{0.94}Ca_{0.06}O_{1.94}$ in multilayer TBC and $Zr_{0.85}Ca_{0.15}O_{1.85}$ in functional graded TBC) was also apparent. This could be related to remaining CMAS glass debris on the top coat surface after the glassification step, prior to the burner rig test. Significantly lower degree of top coat spallation was observed in functional graded TBC, which should be associated with higher GZ endurance against CMAS attack in comparison with the conventional YSZ TBC. Based on the rare earth oxides mechanism of cation substitution with molten CMAS phase, see Poerschke and Levi (2015), the presence of GZ in the YSZ interlayer also plays a substantial role in later formation of slow growing silicates. Moreover, the contribution of the thin top coat in multilayer systems at high temperature cyclic oxidation testing, as also concluded without any detailed explanation of TBCs failure mechanisms in Mahade et al. (2017) and in Gok and Goller (2017), cannot be neglected and future work is needed to explain this effect.

4. Conclusions

Two different thermal barrier coating systems, i.e. multilayer NiCrAlY–YSZ–GZ and functional graded NiCrAlY–YSZ–GZ+YSZ–GZ, were produced by atmospheric plasma spraying. The continuous, thin and dense GZ top coats were formed. The CMAS attack resulted in local flake-like top coat spallation beginning at the top coat free surface and continuing down to the TBC interlayer. The major amount of GZ pyrochlore phase transformed to the zirconium calcium oxide and defect fluorite gadolinium calcium silicate phases. Significantly lower weight loss was observed for functional graded system, in which case GZ in the YSZ interlayer contributed to enhance the TBCs endurance.

Acknowledgements

The research was carried out under the project Research Center of Surface Treatment TE02000011 with financial support from the Technology Agency of the Czech Republic.

References

Bose, S., 2007. Thermal Barrier Coatings (TBCs), in *"High Temperature Coatings"*. In: Jordan Hill, R. (Ed.). Elsevier, Oxford, pp. 299.

Čelko, L., Jech, D., Komarov, P., Remešová, M., Dvořák, K., Šulák, I., Smetana, B., Obrtlík, K., 2017. Failure mechanism of yttria stabilized zirconia atmospheric plasma sprayed thermal barrier coatings subjected to calcia-magnesia-alumino-silicate environmental attack. Solid State Phenomena 270, 39-44.

Darolia, R., (2013). Thermal barrier coatings technology: critical review, progress update, remaining challenges and prospects. International Materials Reviews 58, 315-348.

Drexler, J.M., Ortiz, A.L., Padture, N.P., 2012. Composition effects of thermal barrier coating ceramics on their interaction with molten Ca-Mg-Al-silicate (CMAS) glass. Acta Materialia 60, 5437-5447.

Gok, M.G., Goller, G., 2017. Microstructural characterization of GZ/CYSZ thermal barrier coatings after thermal shock and CMAS+hot corrosion test. Journal of the European Ceramic Society 37, 2501-2508.

Krause, A.R., Garces, H.F., Dwivedi, G., Ortiz, A.L., Sampath, S., Padture, N.P., Calcia-magnesia-alumino-silicate (CMAS)-induced degradation and failure of air plasma sprayed yttria stabilized zirconia thermal barrier coatings. Acta Materialia 105, 355-366.

Lavasani, H.Q., Valefi, Z., Ehsani, N., Masoule, S.T., 2019. Studying the effect of spraying parameters on the sintering of YSZ TBC using APS method. Surface and Coatings Technology 360, 238-246.

Mahade, S., Curry, N., Björklund, S., Markocsan, N., Nylén, P., Vaßen, R., 2017. Functional performance of $Gd_2Zr_2O_7$/YSZ multi-layered thermal barrier coatings deposited by suspension plasma spray. Surface and Coatings Technology 318, 208-216.

Padture, N.P., Gell, M., Jordan, E.H., 2002. Thermal barrier coatings for gas-turbine engine applications. Science 296, 280-284.

Poerschke, D.L., Jackson, R.W., Levi, C.G., Silicate deposit degradation of engineered coatings in gas turbines: progress towards models and materials solutions. Annual Review of Materials Research 47, 297-330.

Poerschke, D.L., Levi, C.L., 2015. Effects of cation substitution and temperature on the interaction between thermal barrier oxides and molten CMAS. Journal of the European Ceramic Society 35, 681-691.

Schulz, U., Braue, W., 2013. Degradation of $La_2Zr_2O_7$ and other novel EB-PVD thermal barrier coatings by CMAS (CaO-MgO-Al_2O_3-SiO_2) and volcanic ash deposits. Surface Coatings and Technology 235, 165-173.

Steinke, T., Sebold, D., Mack, D.E., Vaßen, R., Stöver, D., 2010. A novel test approach for plasma-sprayed coatings tested simultaneously under CMAS and thermal gradient cyclic conditions. Surface and Coatings Technology 205, 2287-2295.